A Unified Linear Fitting Approach for Singular and Non-Singular 3D Quadrics from Occluding Contours

Kongbin Kang
Division of Engineering
Brown University
Providence, RI 02912
Kongbin_Kang@brown.edu

Jean-Philippe Tarel
INRIA, B.P. 105 Rocquencourt
78153 Le Chesnay Cedex
France
Jean-Philippe.Tarel@inria.fr

David B. Cooper
Division of Engineering
Brown University
Providence, RI 02912
cooper@lems.brown.edu

Abstract

A theory and low computational cost linear algorithm is presented for estimating algebraic surfaces of second degree for representing an object in 3D, based on fitting in the dual space (space of tangent planes) computed from images taken by a calibrated camera in a number of positions. The approach and algorithm are designed to handle implicit quadric surfaces, which are regular or singular, in a uniform way without distinguishing the two cases. A significance of these quadric surface estimation results is, as illustrated in the paper, the estimation of complex 3D free form shapes in a computationally simple way in terms of quadric patches. The paper explains how singular quadrics cause instabilities in the 3D surface fitting and representation, and presents regularization, based on this understanding, to produce accurate stable surface representations.

1. Introduction

Many algorithms in computer vision are based on geometric or algebraic approaches that work well for most data configurations but not for some because they result in singularities in the equations being solved. A difficulty arises because in singular cases, perturbing-noise, or outliers or missing data usually produce large erroneous variations in the solutions. The challenge then is to design a unified system that produces stable accurate solutions for both cases by regularizing the equations. For many problems, including those in this paper, that requires understanding the sources of the instabilities and tailoring the regularization to those sources.

We focus here on 3D surface reconstruction from occluding contours in images taken by a moving camera. Developments of this 3D reconstruction problem started assuming a known and small camera motion [4, 2]. Then another kind of approach was proposed in [8, 3, 10, 9] where camera motion can be large between views, but where the occluding contour is assumed cleanly extracted from the images. It is in [11] that the question of optimally combining all the available measurements for better robustness to noise is tackled and partially solved. Another way to achieve robustness to noise and missing data is to use the concept of dual spaces [8, 3, 6]. In [8] and then [3], the dual concept was introduced for computing an algebraic description of quadratic apparent contours in the image of a quadratic surface, and based on the fitted apparent contours the quadric surface can be reconstructed. Taking a very different approach, 3D reconstruction from occluding contours can be reformulated as a fitting problem in the dual space directly. This new approach give us the following benefits: 1) we can work with the raw data in the dual space, i.e., a quadric surface is fit directly to the raw local tangent estimates. Thus, in each image we can use an estimated tangent line at only one point on the apparent contour or at many points on the apparent contour where these points may lie along disconnected curve segments – it does not matter. We use tangent lines wherever we can estimate good edges. However, for the other approach based on fitting quadric curves to apparent contours, the covariances of the coefficients of a fitted quadratic curve, hence, a measure of the accuracy of the fitted curve, are not used. Therefore, high variance quadratic curve coefficients, such as those occurring when a quadratic curve is fit to a short roughly straight line apparent contour, introduce large errors in the computed quadric surface patch. Hence, our fit should be much more accurate in general. 2) We have an automatic way for handling both singular and regular cases. 3) We have a computationally fast way for estimating high order complicated algebraic surfaces from quadric patches.

In [6], this property is explained and a *dual linear fitting algorithm* to 3D reconstruct non-singular algebraic surfaces is introduced.

In this paper, we significantly improve [6] in two ways:

1) We propose a regularization technique to achieve a unified algorithm to dual reconstruct both regular and singular quadrics, 2) We change the eigen fitting approach to a linear system fitting approach, which improves the stability greatly.

Sec. 2 summarizes the dual fitting algorithm for 3D reconstruction of quadrics from occluding contours. Then, the causes of error amplification are analyzed for quadrics in Sec. 3. Two regularization schemes based on Ridge Regression and gradient control are used to achieve stable results, as described in Sec. 4. Then, experiments illustrate the properties of the proposed algorithms on synthetic and real data sets.

2. Dual Fitting for 3D Reconstruction

In this section, we briefly summarize the approach [6] for non-singular quadrics.

2.1. Polynomials and Algebraic Surfaces

To avoid confusion in notation, we start with a few relevant definitions which are used generally in the algebraic geometry literature [1].

Definition 1 *An n-**th degree polynomial** f_n with coefficients in a field k of dimension d is a finite linear combination (with coefficients in k) of n-th degree monomials. We will write such a polynomial f_n in the form:*

$$f_n(X) = \sum_{\{\alpha:\alpha_1+\cdots+\alpha_d \leq n\}} a_\alpha X^\alpha$$

where the sum is over a finite number of d-tuples $\alpha = (\alpha_1, \cdots, \alpha_d)$, with $X^\alpha = \prod_{1\leq i\leq d} x_i^{\alpha_i}$. The set of all polynomials in $X = (x_1, \ldots, x_d) \in k^d$ with coefficients in k is denoted $k[x_1, \cdots, x_d]$.

In computer vision applications, k is usually the real field $k = \mathbb{R}$, i.e, polynomial coefficients are real numbers. For example, a sphere centered at (a, b, c) with radius r in 3D can be described as a second degree polynomial $f(x, y, z) = \sum_{\{\alpha:\alpha_1+\cdots+\alpha_d\leq n\}} a_{ijk}x^i y^j z^k = x^2 + y^2 + z^2 - 2ax - 2by - 2cz + a^2 + b^2 + c^2 - r^2$. In order to made clear the linear property of the polynomial coefficients, we rewrite any polynomial as an inner product of two vectors:

$$f_n(X) = \sum_{\{\alpha:\alpha_1+\cdots+\alpha_d\leq n\}} a_\alpha X^\alpha = A^t Y$$

where A is the coefficient vector and Y is the ordered monomial vector. Let us now formally introduce algebraic curves and surfaces.

Definition 2 *Let $f_1, f_2, \cdots, f_s$ be polynomials in $\mathbb{R}[x_1, \cdots, x_d]$. Then, we set:*

$$V(f_1, \cdots, f_s) = \{X \in \mathbb{R}^d : f_j(X) = 0, 1 \leq j \leq s\}. \quad (1)$$

*$V(f_1, \cdots, f_s)$ is named the **affine variety** defined by $f_1, \cdots, f_s$.*

In 2D or 3D, when $s = 1$, the previously defined affine variety, which is the zero set of a 2D or 3D polynomial, is also named a 2D algebraic curve or a 3D algebraic surface.

2.2. Algebraic Fitting

In practice, data sets are samples, and thus a fitting algorithm is required for estimating which variety best approximates the data set. We assume a given data set of points $X_i \in \mathbb{R}^d, i = 1, \cdots, m$, and a variety $V(f_n)$ defined by only one polynomial f (i.e $s = 1$). If these points do not lie exactly on the variety due to the presence of noise, a classical approach is to apply a least-squares fitting to get parameter vector A by minimizing the following "algebraic" error:

$$e_{algebraic} = \sum_{i=1}^{m} (f_n(X_i))^2 = \sum_{i=1}^{m} A^t (Y_i Y_i^t) A$$

Usually to avoid the trivial zero solution, the constrain $\|A\| = 1$ is added into the previous minimization, and thus coefficient vector A of the fitted polynomial is obtained as the solution of:

$$A = \arg\min \left\{ A^t \sum_{i=1}^{m} Y_i Y_i^t A + \lambda(A^t A - 1) \right\} \quad (2)$$

where λ is the Lagrange multiplier of the constraint.

2.3. Dual Fitting

Given a calibrated camera, we focus on the problem of 3D reconstruction from 2D images seen as a fitting problem [6].

Given a line tangent to the occluding contour in the image, the plane tangent to the surface we want to reconstruct can be easily estimated from the calibration matrix. These tangent planes are a subset of all the planes tangent to the surface we want to reconstruct. But a 3D smooth surface can be defined as the set of 3D points on its surface as well as the set of its tangent planes. Our approach is based on this duality property.

To be more concise, *dual spaces* are defined by:

Definition 3 *Let E be a vector space over $\mathbb{R}$. The algebraic **dual space** E^* is defined to be the set of all linear functionals $\phi : E \to \mathbb{R}$ with respect to operations:*

$$(\phi + \psi)(e) = \phi(e) + \psi(e)$$

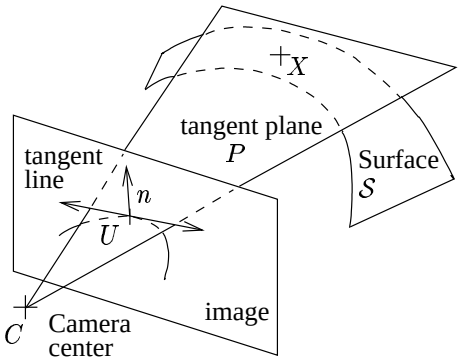

Figure 1. A tangent plane of a 3D point X to the surface $\mathcal{S}$.

$$(\lambda\phi)(e) = \lambda\phi(e)$$

whatever $\lambda \in \mathbb{R}$, $e \in E$ *and* $\phi, \psi \in E^*$.

From definition 3, the set of all 3D affine planes Π is the dual of the real 3D space extended with homogeneous coordinates. Although the above definition is valid for all the tangent planes, in the problem of 3D reconstruction from images only the tangent planes to the convex part can be obtained.

Using the dual space instead of the primal space has an important advantage with respect to the 3D reconstruction: no depth information is needed. To make this point clearer, see Fig. 1 where the tangent plane Π is computed directly from camera center C and tangent line l to the occluding contour. At an image point U of occluding contour (projection on the image of the contour generator of the surface $\mathcal{S}$ to be reconstructed) the tangent line l is computed, and using the camera calibration the normalized tangent plane $P(U)$ of $\mathcal{S}$ is estimated. Since we use homogeneous coordinates, all the 4D points $\mu P(U)$ are points on the manifold $\mathcal{E}$, i.e., dual surface, in dual space formed by all the planes tangent to $\mathcal{S}$. Since there is an isomorphism between the dual space of 3D affine planes and the 3D primal space of points in homogeneous coordinates, this means that the reconstruction of the dual surface $\mathcal{E}$ in the dual space is equivalent to the reconstruction of the surface $\mathcal{S}$ in the primal space.

This means that by working in the space of planes rather than staying in the original 3D space as in the classical approaches, we set the problem as fitting a 4D hyper-surface, i.e., the dual surface $\mathcal{E}$, on 4D data points which represent 3D planes in the original 3D space. When the fitting of $\mathcal{E}$ is performed, any normal to $\mathcal{E}$ gives, up to a scale factor, a point on $\mathcal{S}$. The x, y, z coordinates of the point on $\mathcal{S}$ can by recovered by dividing by the $4th$ component. Thus, $\mathcal{S}$ has been implicitly reconstructed by fitting its dual surface $\mathcal{E}$ in the space of planes. This is how to compute point estimates on $\mathcal{S}$ from the algebraic surface fit in the dual space.

We choose to use the algebraic representation of the 4D surfaces since it leads to linear fitting techniques. The classical and simplest way to fit an algebraic surface to data, as explained in the previous section, is to minimize the algebraic distance over the set of 4D data points (i.e 3D affine planes) $\Pi_i = (p_i, q_i, r_i, s_i)$, $1 \leq i \leq m$, that is

$$e_{algebraic} = \sum_{i=1}^{m} (f_n^*(\Pi_i))^2 = A^{*t} \underbrace{\left(\sum_{i=1}^{m} Y_i^* Y_i^{*t} \right)}_{S^*} A^* \quad (3)$$

using the vector representation of polynomial f_n^* as in (2). The symmetric matrix S^* is the so-called scatter matrix of monomials.

As previously, to avoid the trivial zero solution in the minimization of (3), the constraint $\|A^*\|^2 = 1$ is imposed which modifies the minimization as:

$$A^* = \arg\min \left(A^{*t} \left(\sum_{i=1}^{m} Y_i^* Y_i^{*t} \right) A^* + \lambda(A^{*t} A^* - 1) \right) \quad (4)$$

with the introduction of Lagrange multiplier λ. The solution to (4) is given by the unit eigenvector associated with λ_{min}, the smallest eigenvalue of S^*. In summary, the classical least-squares fitting algorithm consists in computing the scatter matrix S^* of monomials from a set of data planes, and then finding the unit eigenvector of S^* associated with its smallest eigenvalue.

This algorithm works well for non-singular 3D surfaces of degree two (i.e quadrics) when the surface is correctly sampled as shown in [6]. For singular quadrics, special care must be taken because of numerical instabilities.

3. Error Analysis of Dual Fitting of Quadrics

Most data we measured are subject to noise and perturbations. For example, calibration errors and contour detecting errors are always present. These errors will propagate in the dual fitting 3D reconstruction. Hence, it is necessary to analyze how these errors propagate.

3.1. Errors on Computing Tangent Planes

The mapping from the 2D tangent line in the image to the 3D tangent plane to the surface is a linear relation:

$$\Pi = M^t l \quad (5)$$

where Π is the plane parameter vector, l is the tangent line parameter vector and M is the 4×3 projection matrix. Ordinary edge detectors will give us the edge point U and intensity gradient direction n, which can be used to compute

tangent line description l as:

$$l = \begin{pmatrix} n \\ -U^t n \end{pmatrix} \quad (6)$$

Using (5), the tangent plane is described in terms of n and U as:

$$\Pi = M^t \begin{pmatrix} n \\ -U^t n \end{pmatrix} \quad (7)$$

Therefore, the error in estimating tangent plane Π is:

$$\delta\Pi = \delta M^t \begin{pmatrix} n \\ -U^t n \end{pmatrix} + M^t \begin{pmatrix} \delta n \\ -\delta U^t n - U^t \delta n \end{pmatrix} \quad (8)$$

In (8), the plane error consists of two terms: one is due to calibration errors δM, and the other is due to measurement errors δU of the position and δn of the normal of the contour point.

3.2. Error Propagation in Fitting

The propagation of tangent plane errors in the fitting is rather complicated to characterize since the fitting consists of an eigen problem. The theory of perturbations deals with error propagation in such types of eigen problems [7]. Due to the complexity of this theory, we will just outline the fact that the error propagation is related to a decreasing function of the ratios of the other eigen values to the smallest eigenvalue. In practice, due to lack of data, the smallest eigenvalue is close to the other small eigenvalues. In such a case, the fitting is relatively unstable when noise or perturbations are added. Notice that by treating the fitting as a linear fitting problem rather than an eigen problem, more stable fitting can be achieved under noise and missing data using gradient one fitting as described in [12]. In Sec. 4, we discuss how to use the gradient-one regularization technique, to have a more stable fitting of the dual surface in case of noisy and missing data.

3.3. Error Propagation from Dual to Primal Spaces

After the dual surface fit is performed, we have to compute its corresponding primal surface. As explained in [6], the dual surface of a quadric is a quadric, and the primal surface of a dual quadric is also a quadric. More precisely, if D^* is the coefficient matrix of the dual quadric in homogeneous coordinates, the coefficient matrix of the corresponding primal quadric is $D = D^{*-1}$. This inverse is not always well defined when the determinant of D^* is numerically close to zero. Indeed, when the dual quadric D^* is singular (i.e a cone or a cylinder), the primal quadric is also singular. In such case, all the errors on its entries are magnified by the matrix inversion. Following, we use perturbation techniques to quantitatively show error propagation associated with the inverse operation.

An estimated dual quadric coefficient matrix $\hat{D^*}$ can be seen as $\hat{D^*} = D^* + \delta D^*$. D^* is the underlying noiseless dual surface matrix which we want to estimate and δD^* is the error in the dual quadric fitting. Since it is known that for a pair of corresponding primal and dual quadrics $D^* D = I_d$, we deduce:

$$(D^* + \delta D^*) \times (D + \delta D) = I_d$$

where I_d is the identity matrix. Thus, after expansion:

$$D^*\ D + \delta D^*\ \delta D + D^*\ \delta D + \delta D^*\ D = I_d$$

The first term in the left hand side is cancelled by the term in right hand side and second term in the left hand side is a second order smallest term which can be ignored. Thus, we get:

$$D^*\ \delta D + \delta D^*\ D = 0$$

Then using $D = D^{*-1}$. The error on the primal quadric is:

$$\delta D = -D^{*-1}\ \delta D^*\ D^{*-1} \quad (9)$$

From (9) it is clear that fitting errors are amplified during the transformation from the dual space to the primal space when the determinant of D^* is small. This is the main source of numerical instabilities we observed in practice. In Sec. 4, we discuss how to use Ridge-regression regularization techniques in computing D^{*-1} in order to reduce the error amplification effect in the transformation from the dual to primal space without a resulting distortion of the desired fitting result.

3.4. What are Singular Cases?

In this section, we investigate the problem of singularities for algebraic surfaces only. This will help us to intuitively explain the causes of numerical instabilities of the dual fitting algorithm. In the case of explicit surfaces, a singular point (of the first specie) is a surface point where the tangent plane is not defined. In algebraic geometry [1], singular points are usually defined as points on the surface where the gradient of f_n is zero. For us, in the context of dual fitting, a singular point is defined as the following :

Definition 4 *Let $f_n(X) \in \mathbb{R}[x_1, x_2, \cdots, x_d]$ and let $X \in V(f_n)$. The vector of first derivatives of $f_n(X)$, $G_{f_n}(X) = \nabla f_n(X) = (\partial_i f_n(X))$, is called the Gradient vector of f_n at X. Moreover, the matrix of second derivatives of $f_n(X)$, $H_{f_n}(X) = \nabla^t \nabla f_n(X) = (\partial_i \partial_j f_n(X))$, is called the Hessian matrix of f_n at X. The coefficient matrix of the quadric which approximates the algebraic surface arround X is:*

$$D_{f_n}(X) = \begin{bmatrix} f_n(X) & G^t_{f_n}(X) \\ G_{f_n}(X) & H_{f_n}(X) \end{bmatrix}$$

in homogeneous coordinates. Thus:

- *X is a **singular point** of $V(f_n)$ when the approximated quadric matrix $D_{f_n}(X)$ is not full rank.*
- *otherwise, X is a non-singular point of $V(f_n)$*

The previous definition implies that a point X on the surface $(f_n(X) = 0)$ where the gradient $G_{f_n}(X)$ is zero is singular. Thus:

Definition 5 *A **singular surface**, in the context of the dual fitting, is an algebraic surface which contains at least one singular point.*

The idea of the above definitions is that a non-singular surface does not have a dual surface that is locally collapsed in the dual space, i.e, the dual surface maintains a full rank matrix for each quadric approximation at each point all along its surface. For example, as seen previously, among second degree irreducible (non-factorizable) polynomials, cones and cylinders are singular surfaces because the set of tangent planes along cones and cylinders collapses one dimension in the dual space. Both dual shapes lie on hyperplanes in 4 dimensional homogeneous space. They are planar quadric curves in dual space, i.e., degree 2.

From definition 4, we can see that a locally estimated primal surface at a singular point is unstable because of two reasons: 1) in dual space, fitting a surface model to a curve results in an unstable surface fit; 2) computing the gradient of this fitted surface at points in the vicinity of the curve in order to get a surface point in the primal space produces unstable gradients. These difficulties can be illustrated by a simple example. Suppose we have a cone whose tip is at $(0, 0, 0)$, the origin of the reference system in the primal space, i.e., 3D surface, coordinates. Since every tangent plane passes through the tip (approximately for real data), the dual points collapse into a scatter around a curve in a plane which has normal vector $(0, 0, 0, 1)$ in homogeneous coordinates. As shown in Fig. 2, fitting a surface model to data scattered around a curve is an ill-posed problem. Moreover, a normal to the dual surface corresponds to a point on the primal surface, but for singular points, this normal is not uniquely defined. Thus, when we normalize the normal by dividing the normal by it's last component to get a 3D point of the cone, the computed point is far away from its correct value.

To cope with those singular surfaces, the simplest idea is to determine whether the estimated dual surface collapses in dimension. However, this approach requires a detection, and thus a threshold, on dimension collapse, which is difficult to perform since we do not a priori know the correct dual surface. Consequently, in the following sections, we propose a unified dual fitting 3D reconstruction algorithm which doesn't need to distinguish between singular and non-singular cases. The main idea to build such an algorithm is to add few well chosen constraints which will bias singular cases a little towards non-singular cases without modifying the non-singular cases. This approach allows us to drastically stabilize the fit of singular quadrics.

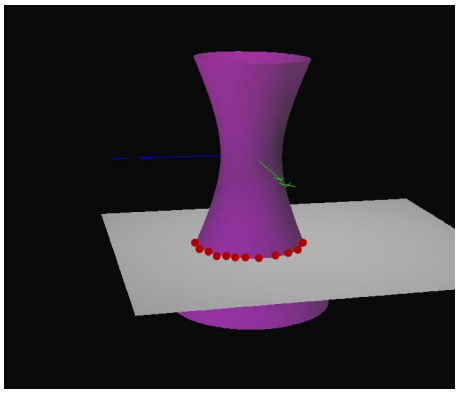

Figure 2. This illustration shows there is ambiguity in fitting a surface to a planar curve data. The red dots are the data points which lie on a plane. When using real data, these points will lie near but off the plane. There is then huge variability in the range of surfaces that fit this scatter-around-the-curve data equally well. One of the possible fitting results, a hyperbolic surface, is shown. This leads to an estimated hyperbolic surface in the primal space, which is a poor representation for the true cone. It is clear that additional information is required to get a meaningful fit.

4. Dual Fitting 3D reconstruction Regularization

As described previously, the problem of unstable 3D reconstruction is due to singular points where locally the surface and its dual surface are singular quadrics. For ill-posed problems no unique solution exists because, in effect, there is not enough information specifying it [13]. To get a meaningful solution, we introduced two kinds of regularizations in the 3D reconstruction algorithm to bias the solution towards non-singular local quadrics. We first introduce a regularization scheme based on scaling and Ridge Regression to stabilize the transformation between the dual and primal space. Second, we propose another scheme based on gradient-one constraint to deal with the problem of dual data collapse in dimension.

4.1. Ridge-Regression for Dual to Primal Transformation

Close to singular points, the local quadric approximating the surface is close to singular. Its quadric coefficient-matrix in homogeneous coordinates has a bad conditioning number, and leads to a badly conditioned inverse matrix [5].

However, if we bias the fitted dual quadric *by adding a well chosen matrix*, we can greatly increase the stability of the primal quadric coefficient-matrix without significantly changing the desired shape.

To begin, every dual data point $\Pi_i = (p_i, q_i, r_i, s_i)$ which represents a tangent plane of the primal surface is normalized to enforce norm one of the tangent plane, i.e $p^2 + q^2 + r^2 = 1$. Then, if the set of normalized $(\Pi_i), 1 \leq i \leq m$ is close to a plane, the primal quadric is a cone or cylinder and thus the normal N to the plane gives the tip of the primal cone or direction of cylinder axis in homogeneous coordinates. Normal N can be simply estimated from the data set (Π_i) by minimizing:

$$N = \arg\min \left\{ N^t \sum_{i=1}^{m} \Pi_i {\Pi_i}^t N \right\} \tag{10}$$

under $\|N\|^2 = 1$. It is a minimum value eigen problem. Notice that after the tip N is estimated, the primal coordinate system origin can be moved to the tip. Then, tangent planes (Π_i) are recomputed in the translated coordinate system. This helps to reduce numerical instabilities by centering the data set before fitting. Before fitting, whitening of matrix $\sum_{i=1}^{m} \Pi_i {\Pi_i}^t$ can also be performed with resulting advantages.

Let D^* denote the dual quadric matrix obtained after fitting. To cope uniformly with both singular and non-singular cases, rather than using $D = {D^*}^{-1}$ as primal quadric matrix, we use:

$$D = \left(D^* + \lambda N N^t\right)^{-1} \tag{11}$$

where λ controls the amount of regularization

Intuitively, $\lambda N N^t$ in the right hand side of (11) pulls the overall primal surface, i.e., the 3D object surface, towards the tip point. Equivalently, for singular cases, as the λ increases, the primal quadric described by (11) better approximates the true singular quadric. For the non-singular case, the effect of $\lambda N N^t$ on D is small if λ is small compared to D^*. This regularization turns out to be appropriate for handling cylinders as well.

4.2. Gradient-One Dual Fitting

Since fitting a curve with a surface model in the dual space is an ill-posed problem, extra information can be added to force the fitting to get the desirable result. For example, in Fig. 2, if we know N the normal of the plane where the dual surface is included, then the hyperboloid is more desirable than the ellipsoid because the ellipsoid has points far away from the plane N.

To force the dual fit to be close to plane N in the neighborhood of the data points, we put soft constraint $\|\nabla f - N\|^2 = 0$ into the fitting algorithm, where N is the normal of the plane going through the data estimated as in the previous section. We can rewrite the above constrains into a differential form which is more convenient to be used in the fitting.

$$0 = \|\nabla f - N\|^2 = A^t \nabla Y \nabla Y^t A - 2N \cdot \nabla Y^t A + 1 \tag{12}$$

When constraint (12) is introduced into the fitting minimization, we get:

$$\begin{array}{rl} A & = \arg\min \{A^t (S + \mu \sum_{i=1}^{m} \nabla Y_i \nabla Y_i^t) A \\ & \quad -2\mu A^t \sum_{i=1}^{m} (N \cdot \nabla) Y_i \ \} \end{array} \tag{13}$$

From definition 4, locally at a singular point, points on the dual surface lie in a planar curve instead of a curved surface, and thus the constraint biases the fit to a close to planar quadric. On the contrary, when the point is non-singular, this constraint does not change the resulting fit much.

With the use of the gradient-one constraint, the solution of the regularized fitting problem, i.e of (13), consists in solving the linear system:

$$A = \left(\sum_{i=1}^{m} Y_i Y_i^t + \mu \nabla Y_i \nabla Y_i^t \right)^{-1} \left[\sum_{i=1}^{m} (N \cdot \nabla) Y_i \right] \tag{14}$$

We call the above fitting algorithm gradient-one dual fitting because the constraint in (13) is close to gradient-one constraint introduced in [12] which was used to increase direct algebraic curve fitting stability in primal space. In [12], the gradient-one constraint used is $(N^t \nabla f - 1)2 + (T^t \nabla f)2 = 0$ which also implies that the gradient of f locally agrees with the data normal at regular points. Therefore, we have applied with success to dual fitting the gradient-one constraint used by [12]. Here, we use only the normal term of the gradient-one constraint. But a basis of the tangent plane to the dual curve at every Π_i can be also easily obtained using information about point U_i on the images as explained in [6].

The main advantage of gradient-one dual fitting over previous eigen dual fitting in [6] is that errors propagate in a better way. Indeed, for gradient-one dual fits, the error analysis can be performed more easily, since the minimization leads to a linear system, instead of an eigen problem.

5. Experiment Results

5.1. Synthetic data experiments

We conducted experiments on synthetic data to show how the gradient one weighting factor μ effects the fitting

results. In the following two experiments we set ground truth surfaces which we want to reconstruct as the ellipsoid $x^2+\frac{1}{4}y^2+\frac{1}{2}z^2=1$ and the cone $x^2-\frac{1}{4}y^2+\frac{1}{2}z^2=0$. The camera is about 1500 millimeters away from the centers of these objects. Then we move the camera to 5 different positions to compute the contours in 5 different images. The baseline between the last camera and the first camera positions is about 500 millimeters. The external parameters are known perfectly. The used internal parameters are the ones of a Nikon 5000 camera at manual focus $f=7.1mm$. After those contour points were generated using ground truth surface parameters and camera internal and external parameters, we used the gradient-one algorithm (see (13)) to estimate the primal surface under different μ.

The results of both experiments are shown in Fig. 3(a) and Fig. 3(b). Figures in Fig. 3 show error changes when gradient-one weighting factor μ increases. In Fig. 3(a), we can see that the computed ellipsoid is biased away from its true shape as μ increases. When $\mu \leq 10^{-4}$ the bias of the reconstructed surface is less than 1%, on its three axes. The bottom figure of Fig. 3(b) shows that the reconstructed shape is closer to a cone as the weighting factor μ increases, but the bias on the reconstructed shape increases as well. The trade-off between increase of the stability and bias of the reconstruction seems correct for a μ around 10^{-4}. This shows that the algorithm we proposed in the Sec. 4 is valid for both non-singular and singular surfaces. Therefore, it can be called "unified dual fitting 3D reconstruction algorithm".

5.2. On the Choice of the λ and μ

The weighting factor, λ, in (11) is set by:

$$\lambda = sign(D_{44})\alpha \min_{i=1,2,3}\{D_{ii}\}$$

where $sign(x)$ is the signum function which is used to avoid changing the fitted shape from a hyperbolic surface to a parabolic surface. α is always set to 2% which guarantee a reconstructed shape bias within 2% and improves the stability of singular shapes greatly.

Fig. 4 shows how the shape changes when α increases. The tip of Fig. 4(a) is much sharper than that of Fig. 4(b). This confirms the discussion in Sec. 4. As α increases, the tip of the reconstructed shape will approach the true value, becoming sharper and sharper. But for non-singular quadrics, reconstructed shape diverges away from the true shape. We noticed that for the funnel, cross section is nearly a circle. But the ratio of the two axes moves away from 1 as λ increases. From the experiment, we also can see that when $\lambda < 10^{-2}$, the ratio changes a little. This justified our setting λ to the fixed value 10^{-4} in the following real experiments. Moreover, the gradient-one weighting factor is set to $\mu = 10^{-4}$ in (13), as explained in the previous section.

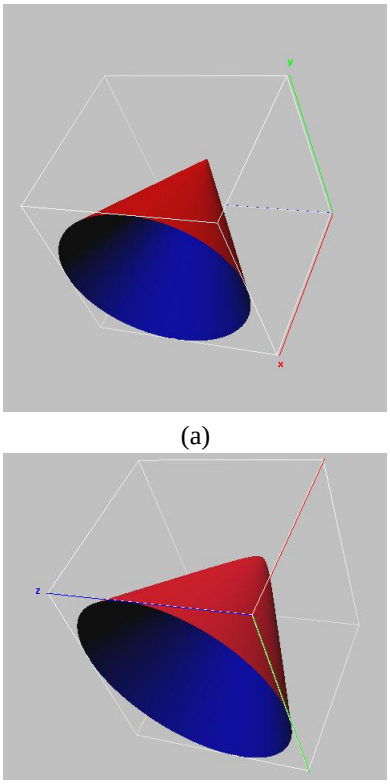

(a) (b)

Figure 4. Different λ effects on the reconstructed shape for a cone. In (a) λ is set to 100% of the shortest axis, and in (b) λ is set to 2% of the shortest axis.

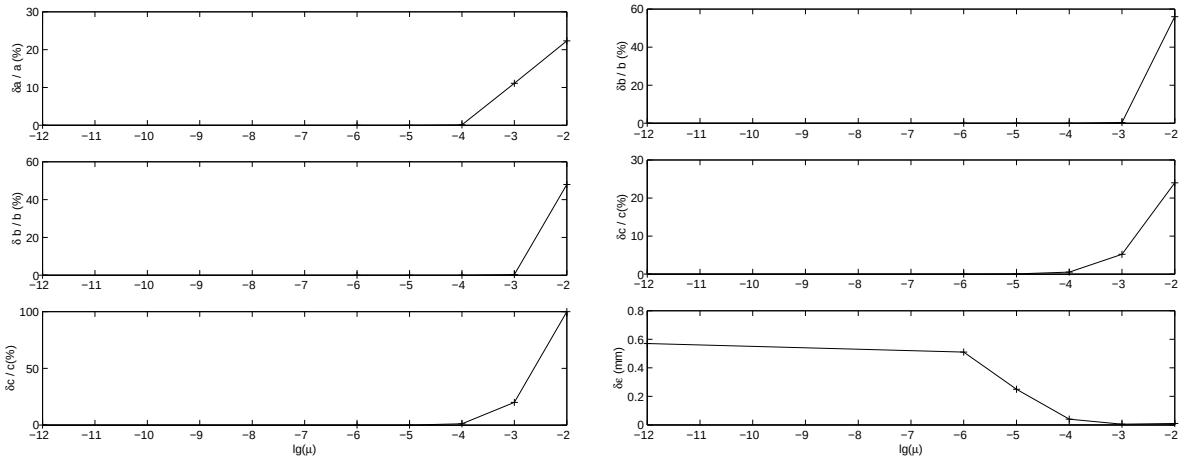

(a) (b)

Figure 3. μ effects on the dual gradient-one reconstruction for a non-singular and a singular quadrics. In column (a), three curves display the μ effect on ellipsoid axis lengths, a, b, c, respectively. x-axis is $\log(\mu)$ and y-axis is the relative error. In column (b), the reconstructed primal surface is a hyperboloid having axis z and elliptic cross-section; the three curves display the μ effect on cross-section ellipse axes lengths at $z = 1$, and bottom, on the distance of the hyperboloid to the true tip position of the cone.

5.3. 3D Reconstructions Based on Real Data

We performed real experiments to test the 3D reconstruction dual algorithm proposed in Sec. 4. In these experiments, different objects are used with a Nikon 5000 digital camera. The camera is posed at about 1200 millimeters away from the center of the object. Then we moved the camera to different positions to take images. Contours are extracted from images using the Canny edge detector. The baseline between the last camera and the first cameras is about 700 millimeters. We use Zhang's camera calibration algorithm [14] to calibrate camera internal and external parameters.

Fig. 5 shows the setup of the gradient one fitting experiment on a singular shape (a cone) and the 3D reconstruction. In Fig. 5(a), the funnel which we want to reconstruct is placed right under a planar calibration board which is used to calibrate camera parameters. We see from the image that the shape is close enough to a cone.

Fig. 6 shows a cylindrical box for experiment and the reconstruction. Although a cylinder is a singular shape, the proposed dual fitting algorithm can reconstruct it well.

Fig. 7(b) illustrates a 4th degree algebraic surface estimated from occluding contours in 7 views of the sculpture shown in Fig. 7(a). 3D primal space is partitioned into large cubes, a dual quadric surface is estimated in each cube using the algorithm in this paper, then points are sampled from the primal surface for each of the estimated dual quadric surfaces, and a single 4th degree algebraic surface is fit to these sampled points. See [6] for a discussion of this data and reconstruction but using the original dual quadric surface estimator in [6] rather than the improved quadric surface estimator in this present paper.

6. Conclusion and Outlooking

We proposed a new stable low-computational-cost linear fitting algorithm for 3D surface reconstruction from occluding contours. The analysis of the causes of trouble in dual fitting allows us to propose an algorithm which handles shapes with and without singular parts in a unified way without distinguishing the existing singularity case or cases. For quadric surface, singular surfaces are the cone and the cylinder. We illustrate the practical effectiveness of the approach on real and synthetic data. These are major extensions of the algorithms in [6].

Acknowledgements

This work was partially supported by NSF Grants IIS-0205477 and IIS-9802392.

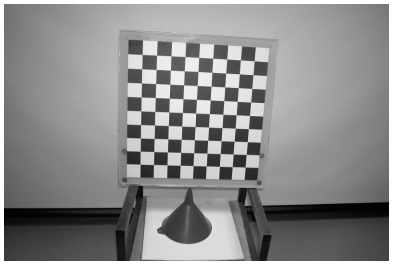

(a)

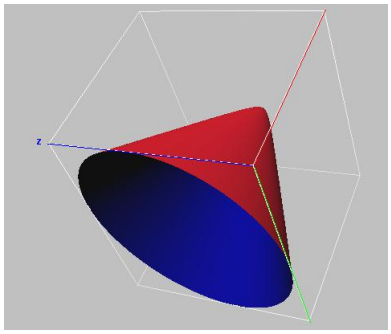

(b)

Figure 5. (a) one of 8 images used for funnel reconstruction. (b) the 3D model computed using dual fitting 3D reconstruction algorithm.

(a)

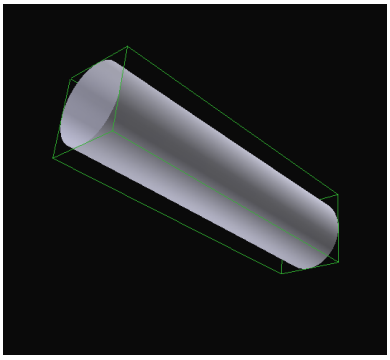

(b)

Figure 6. (a) one of 7 images used for reconstruction. (b) the 3D model computed using the dual fitting 3D reconstruction algorithm

References

[1] D. Cox, J. Little, and D. O'Shea. *Ideals, Varieties, and Algorithms: an introduction to computational algebraic geometry and commutative algebra*. Springer-Verlag New York, Inc., 1st edition, 1991.

[2] G. Cross, A. Fitzgibbon, and A. Zisserman. Parallax geometry of smooth surfaces in multiple views. In *ICCV*, pages 323–329, 1999.

[3] G. Cross and A. Zisserman. Quadric surface reconstruction from dual-space geometry. In *Proc. 6th International Conference on Computer Vision*, pages 25–31, Bombay, India, January 1998.

[4] P. Giblin and R. Weiss. Reconstructions of surfaces from profiles. In *International Conference on Computer Vision*, pages 136–144, 1987.

[5] A. Hoerl and R. Kennard. Ridge regression: Biased estimation for nonorthogonal problems. *Technometrics*, 12(3):55–67, 1970.

[6] K. Kang, J.-P. Tarel, R. Fishman, and D. B. Cooper. A linear dual-space approach to 3d surface reconstruction from occluding contours using algebraic surface. In *International Conference on Computer Vision*, volume 1, pages 198 – 204, Vancouver, Canada, 2001.

[7] T. Kato. *A Short Introduction to Perturbation Theory for Linear Operators*. Springer-Verlag, 1980.

[8] S. Ma and L. Li. Ellipsoid reconstruction from three perspective views. In *International Conference on Pattern Recognition*, page A8M.5, 1996.

[9] P. Mendonca, K. Wong, and R. Cipolla. Camera pose estimation and reconstruction from image profiles under circular motion. In *European Conference on Computer Vision*, pages II: 864–877, 2000.

[10] S. Sullivan and J. Ponce. Automatic model construction and pose estimation from photographs using triangular splines. *IEEE Transactions on Pattern Analysis and Machine Intelligence*, 20(10):1091–1096, October 1998.

[11] R. Szeliski and R. Weiss. Robust shape recovery from occluding contours using a linear smoother. *International Journal of Computer Vision*, 28(1):27–44, June 1998.

[12] T. Tasdizen, J.-P. Tarel, and D. B. Cooper. Improving the stability of algebraic curves for applications. *IEEE Transactions on Image Processing*, 9(3):405–416, March 2000.

[13] A. N. Tikhonov and V. Y. Arsenin. *Solutions of ill-posed Problems*. Winston, Washington, 1977.

[14] Z. Zhang. A flexible new technique for camera calibration. *PAMI*, 22(11):1330 – 1334, 2000.

(a)

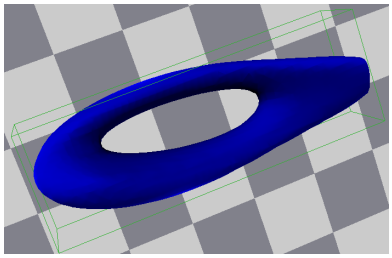

(b)

Figure 7. (a) the sculpture used for reconstruction. (b) the $4th$ degree polynomial 3D model computed using the dual fitting 3D reconstruction algorithm. The measured data was that used by authors in [6].